Inorganic Chemistry

Article

pubs.acs.org/IC

UV Nonlinear Optical Crystal $Ba_2[B_6O_9(OH)_4]$ Featuring Unique Chiral Layers with a New $B_{18}O_{42}$ Circle Based on BO_3 and BO_4 Units

Li Wang,[†,‡] Shilie Pan,*[,†] Lixian Chang,[‡] Jianyang Hu,[‡] and Hongwei Yu[†]

[†]Xinjiang Key Laboratory of Electronic Information Materials and Devices, Xinjiang Technical Institute of Physics & Chemistry, Chinese Academy of Sciences, 40-1 South Beijing Road, Urumqi 830011, China

[‡]College of Chemistry and Chemical Engineering, Xinjiang Normal University, Urumqi 830054, China

Supporting Information

ABSTRACT: A new noncentrosymmetric polyborate, $Ba_2[B_6O_9(OH)_4]$, has been synthesized under a hydrothermal condition. The polyborate contains chiral layers constructed by two kinds of helical chains and also form new $B_{18}O_{42}$ circles based on B_3O_8 units [(3: Δ+2T)]. One kind of Ba atom locates in the cavity surrounded by the $B_{11}O_{11}$ ring within the anion layer, and the other kind of Ba atom inserts between two adjacent layers. UV−vis diffuse reflectance spectroscopy demonstrates that the compound has a cutoff edge below 190 nm and has a large second-harmonic generation (SHG) effect, which is approximately 3 times that of KH_2PO_4 (KDP) and is type-I phase matchable.

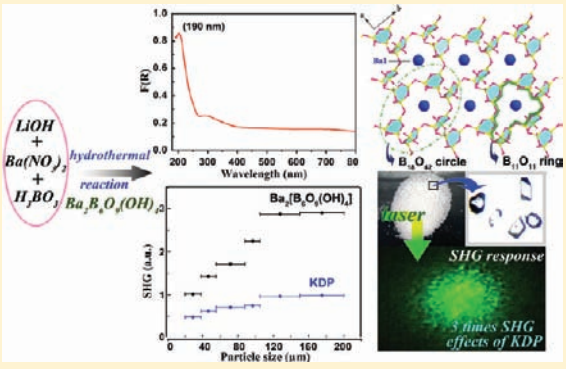

INTRODUCTION

Nonlinear optical (NLO) materials have played an important role in laser science and technology.[1−12] Some typical NLO materials, such as β-BaB_2O_4 (BBO),[8] LiB_3O_5 (LBO),[9] CsB_3O_5 (CBO),[10] $CsLiB_6O_{10}$ (CLBO),[11] and $AgGaS_2$,[12] have been used extensively. However, it is still a challenge to entirely meet the needs of the large second-harmonic generation (SHG) coefficient, wide transparent range, moderate laser damage threshold, and phase matchability for the increasingly expanding field. Thus, understanding the correlation among the composition, structure, and NLO properties of crystals is still critical in exploring new SHG materials with better performance. As a remarkable source of the NLO material, borates have distinctive advantages, such as the large SHG, excellent UV transmittance, and high damage threshold value, etc.[4−6,8−12] Acccording to the theory of anion groups by Chen et al., the large SHG may result from inorganic borate π-orbital systems, such as $[B_3O_6]^{3-}$ in β-BaB_2O_4 (BBO) and $[B_3O_7]^{5-}$ in LiB_3O_5 (LBO).[8,9] In fact, the diversity of the borates crystal chemistry still allows us to obtain new borates with SHG properties and also provides new opportunities to probe the structure−property relation. On the other hand, the cationic effects of the NLO materials received increasing attention; the SHG activity increases with the ionic distortion or polarization of the cation, such as the isostructural pentaborates $M_2B_5O_9X$ (M = Ca, Sr, Ba; X = Cl, Br and I) and shows an activity order of Ca < Sr < Ba.[5c] Furthermore, the alkali metal−oxygen bond is ideal for transmission of UV light because there are no electron transitions in this range.[6,8−12] In particular, the rational combination of possible multiple types of units in the same compound is an effective synthetic route for new inorganic solids with excellent SHG properties if those units are properly aligned.[5,6] Inspired by the above principles, we expect that combining the borate groups with the barium ions will generate new kinds of UV NLO materials. Here we report the preparation of $Ba_2[B_6O_9(OH)_4]$, a new NLO crystal featuring chiral layers with unique $B_{18}O_{42}$ circles based on BO_3 and BO_4 units, showing a SHG activity of about 3 times that of KDP.

EXPERIMENTAL SECTION

Synthesis. All of the chemicals were analytically pure, received from commercial sources, and used without further purification. A mixture of $Ba(NO_3)_2$ (1.045 g, 4.0 mmol), H_3BO_3 (0.185 g, 3.0 mmol), $LiOH·H_2O$ (0.020 g, 0.5 mmol), and H_2O (10.0 mL) was sealed in an autoclave equipped with a Teflon linear (23 mL) and heated at 200 °C for 3 days, followed by slow cooling to room temperature at a rate of 4 °C/h. The product was washed with water and then dried in air. Colorless block-shaped crystals of $Ba_2[B_6O_9(OH)_4]$ were obtained in a yield of ca. 85% based on Ba. Interestingly, the synthesis of $Ba_2[B_6O_9(OH)_4]$ relies on subtle control over various hydrothermal parameters, especially introduction of LiOH, which may act as a effective base to form the tetrahydroxyborate ion: $B(OH)_3 + H_2O = B(OH)_4^- + H^+$. Having a more electron-donating group, $B(OH)_4^-$ has higher reaction activity than $B(OH)_3$. The initial pH values were 8−9, and final pH values were 7 of the reaction media. Therefore, it can be reasonably speculated that LiOH is the necessary acid−base buffer in the synthesis processing of $Ba_2[B_6O_9(OH)_4]$.

X-ray Crystallographic Studies. The crystal structure of $Ba_2[B_6O_9(OH)_4]$ was determined by single-crystal X-ray diffraction on an APEX II CCD diffractometer using monochromatic Mo Kα

Received: October 2, 2011
Published: January 19, 2012

   dx.doi.org/10.1021/ic2021337 | Inorg. Chem. 2012, 51, 1852−1858

radiation (λ = 0.71073 Å) at 296(2) K and intergrated with the SAINT program.[13] A colorless and transparent crystal with dimensions of 0.24 × 0.18 × 0.09 mm^3 was chosen for structure determination. All calculations were performed with programs from the SHELXTL[14] crystallographic software package. The positions of non-hydrogen atoms were refined using full-matrix least-squares techniques with anisotropic thermal parameters. Final least-squares refinement on F_o^2 with data having $F_o^2 \geq 2\sigma(F_I^2)$ includes anisotropic displacement parameters for non-hydrogen atoms. The final difference Fourier synthesis map shows the maximum and minimum peaks at 1.591 and −1.481 e·Å^{-3}, respectively. The hydrogen atoms bonded to O1, O6, O12, and O13 atoms are located from the electron density map. The structure is checked for missing symmetry elements with PLATON.[15] Crystal data and structure refinement information is given in Table 1;

Table 1. Crystal Data and Structure Refinement for $Ba_2[B_6O_9(OH)_4]$

empirical formula	$Ba_2[B_6O_9(OH)_4]$
fw	551.57
temp.	296(2) K
wavelength	0.71073 Å
cryst syst	monoclinic
space group, Z	$P2_1$, 2
unit cell dimens	a = 6.828(2) Å
	b = 8.706(3) Å
	c = 8.441(3)Å
	β = 100.615(3)
vol.	493.2(3) Å^3
density (calcd)	3.714 Mg/m^3
abs coeff	8.015/mm
F(000)	500
cryst size	0.24 mm × 0.18 mm × 0.09 mm
theta range for data collection	2.45−27.57°
limiting indices	$-7 \leq h \leq 8$, $-11 \leq k \leq 6$, $-10 \leq l \leq 10$
reflns collected/unique	2892/1687 [R(int) = 0.0352]
completeness to theta = 27.57	98.8%
refinement method	full-matrix least-squares on F^2
data/restraints/params	1687/35/200
goodness-of-fit on F^2	1.146
final R indices [$F_o^2 > 2\sigma(F_o^2)$]^a	R_1 = 0.0287, wR_2 = 0.0708
R indices (all data)^a	R_1 = 0.0288, wR_2 = 0.0709
Flack parameter	0.04(3)
extinction coeff	0.0134(13)
largest diff. peak and hole	1.591 and −1.481 e·Å^{-3}

$^a R_1 = \sum||F_o| - |F_c||/\sum|F_o|$ and $wR_2 = [\sum w(F_o^2 - F_c^2)^2/\sum w F_o^4]^{1/2}$ for $F_o^2 > 2\sigma(F_o^2)$.

selected bond distances are listed in Table 2. Final coordinates and equivalent isotropic displacement parameters of the non-hydrogen atoms, selected bond bond angles (deg), and hydrogen bonds (Angstroms) are listed in Tables S1, S2, and S3, Supporting Information, respectively.

X-ray Powder Diffraction. X-ray powder diffraction analysis of $Ba_2[B_6O_9(OH)_4]$ was performed at room temperature in the angular range of 2θ = 10−70° with a scan step width of 0.02° and a fixed counting time of 1s/step using an automated Bruker D8 ADVANCE X-ray diffractometer equipped with a diffracted beam monochromator set for Cu Kα radiation (λ = 1.5418 Å). The powder X-ray diffraction pattern of $Ba_2[B_6O_9(OH)_4]$ is in good agreement with that calculated derived from the single-crystal data and is shown in Figure S1, Supporting Information.

Infrared Spectroscopy. An infrared spectrum was recorded on Shimadzu IR Affinity-1 Fourier transform infrared spectrometer in the range from 400 to 4000 cm^{-1} with a resolution of 2 cm^{-1}. The 6 mg of sample was mixed thoroughly with 500 mg of dried KBr.

Table 2. Selected Bond Distances (Angstroms) for $Ba_2[B_6O_9(OH)_4]$[a]

B1—O2	1.460(8)	Ba1—O9^i	2.639(5)
B1—O1	1.457(9)	Ba1—O4	2.766(5)
B1—O3	1.484(9)	Ba1—O8^i	2.773(5)
B1—O4^a	1.506(9)	Ba1—O7^a	2.803(5)
B2—O5	1.360(9)	Ba1—O6^j	2.801(5)
B2—O4	1.385(10)	Ba1—O2	2.803(5)
B2—O3	1.389(10)	Ba1—O1	2.874(5)
B3—O7	1.463(9)	Ba1—O3^b	2.896(5)
B3—O2^b	1.459(9)	Ba1—O12^k	2.959(6)
B3—O6	1.467(8)	Ba1—O13^a	3.124(5)
B3—O5	1.510(9)	Ba2—O2	2.764(5)
B4—O7	1.438(9)	Ba2—O12^d	2.809(6)
B4—O11^d	1.465(8)	Ba2—O13^l	2.834(6)
B4—O8	1.485(9)	Ba2—O8^j	2.856(5)
B4—O9	1.519(9)	Ba2—O11^l	2.861(5)
B5—O8^g	1.348(9)	Ba2—O9^m	2.941(5)
B5—O10	1.359(8)	Ba2—O5^j	2.949(5)
B5—O9	1.377(9)	Ba2—O6^j	3.008(6)
B6—O11	1.453(9)	Ba2—O10^d	3.036(5)
B6—O12	1.456(9)	Ba2—O3	3.080(5)
B6—O13	1.475(10)	Ba2—O4	3.120(5)
B6—O10	1.517(9)		

[a]Symmetry codes: (a) 1 − x, 0.5 + y, 1 − z; (b) 1 − x, −0.5 + y, 1 − z; (c) 1 + x, y, z; (d) 2 − x, 0.5 + y, 2 − z; (e) 1 + x, y, z + 1; (f) 1 − x, −0.5 + y, 2 − z; (g) 2 − x, −0.5 + y, 2 − z; (h) 1 + x, −1 + y, z; (i) −1 + x, y, −1 + z; (j) −1 + x, y, z; (k) 2 − x, 0.5 + y, 1 − z; (l) −1 + x, 1 + y, z; (m) 1 − x, 0.5 + y, 2 − z; (n) 2 − x, −0.5 + y, 1 − z.

UV−Vis Diffuse Reflectance Spectrum. Optical diffuse reflectance spectrum was measured at room temperature with a Shimadzu SolidSpec-3700DUV spectrophotometer. Data were collected in the wavelength range 190−800 nm.

TGA/DSC Analysis. The TGA/DSC curve was carried out on a simultaneous NETZSCH STA 449F3 thermal analyzer instrument with a heating rate of 10 °C min^{-1} in an atmosphere of flowing N_2 from 40 to 600 °C.

Second-Order NLO Measurements. The noncentrosymmetric structure of $Ba_2[B_6O_9(OH)_4]$ prompts us to measure its SHG properties. The test was performed on microcrystalline samples of $Ba_2[B_6O_9(OH)_4]$ by the Kurtz−Perry method.[16] Because the SHG efficiency has been shown to depend on particle size, polycrystalline $Ba_2[B_6O_9(OH)_4]$ was ground and sieved into distinct particle size ranges: <20, 20−38, 38−55, 55−88, 88−105, 105−150, and 150−200 μm. Fundamental 1064 nm light was generated with a Q-switched Nd:YAG solid-state laser (1064 nm, 10 kHz, 10 ns). The intensity of the frequency-doubled output emitted from the sample was measured using a photomultiplier tube. The microcrystallines of KDP served as the standard and were sieved into the same particle size ranges.

RESULTS AND DISCUSSIONS

Crystal Structure. $Ba_2[B_6O_9(OH)_4]$ crystallizes in the polar space group $P2_1$ with an asymmetric unit consisting of 2 Ba atoms, 6 B atoms, 13 O atoms, and 4 H atoms (Figure 1). Crystallographic analysis reveals that $Ba_2[B_6O_9(OH)_4]$ contains unique infinite layers $[B_6O_9(OH)_4]_n^{4n-}$ extended by the B_3O_8 units made up of one BO_3 triangle (Δ) and two BO_4 tetrahedra (T) with vertex-sharing O atoms along the ab plane. It is worthy to be noticed that although B_3O_8 units are made up of one BO_3 triangle and two BO_4 tetrahedra, there are two different spatial connections. As shown in Figure 2, the type A B_3O_8 units connect to the adjacent B_3O_8 units through O3a, O7 of two different BO_4 tetrahedra and O3 of one BO_3 triangle

dx.doi.org/10.1021/ic2021337 | Inorg. Chem. 2012, 51, 1852−1858

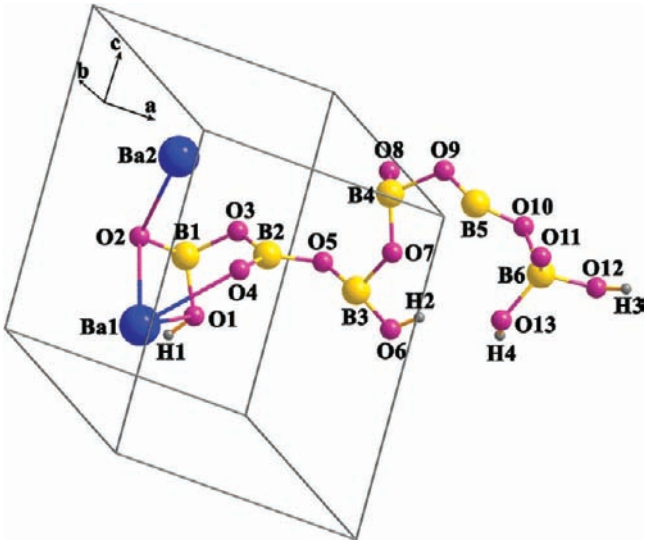

Figure 1. Asymmetric unit of $Ba_2[B_6O_9(OH)_4]$.

while the type B B_3O_8 units connect to the adjacent B_3O_8 units through O7, O9a atoms of the same BO_4 tetrahedron and O9 atoms of one BO_3 triangle. In fact, the above two types of units organize two different unidimensional helical chains, respectively (chain A and chain B, Figure 3), that run parallel to the *b* axis. Furthermore, a homochiral layer was formed by the alternately arranged helical chains, linked uniformly together by interchain oxygen atoms. Within the layer, with an AAABBB cyclization manner, three units of A and three units of B form a new $B_{18}O_{42}$ circle 18: 6 [(3: Δ+2T)], according to the definition given by Christ et al.[17] Although the B_nO_m groups in borates are well documented,[18−21] such layer containing $B_{18}O_{42}$ circles is extremely rare in both hydrated and anhydrous borates. The triangularly coordinated boron atoms have B−O distances in the range 1.348(9)−1.389(10) Å [average = 1.370(7) Å], and the tetrahedrally coordinated B atoms have longer B−O distances in the range of 1.438(9)−1.519(9) Å [average = 1.476(7) Å]. The above values are in agreement with other borate compounds reported previously.[22] The Ba1 atom is located in the cavity surrounded by the $B_{11}O_{11}$ ring within the $B_{18}O_{42}$ circles of anion layer, while the Ba2 atom is located between two adjacent layers to form the 3D structure (Figure 4). As shown in Figure 5, Ba1 atom is surrounded by 10 O atoms, in which there are 9 of the Ba−O distances in the range of 2.639(5)−2.959(6) Å, and bonding to the O13 atom with a significantly longer distance of 3.124(5) Å. The Ba2 atom is surrounded by 11 O atoms, in which there are 10 of the Ba−O distances in the range of 2.764(5)−3.080(5) Å, and bonding to the O2 atom with a significantly longer distance of 3.120(5) Å. At the same time, there are hydrogen bonding O1−H1···O11 [2.726(7) Å] in the same anion layer along with the interlayer hydrogen-bonding interactions O6−H2···O1 [3.104(7) Å)], O12−H3···O9 [2.964(8) Å], O12−H3···O10 [2.964(8) Å], and O13−H4···O1 [2.921(8) Å], which lead to a tight 3D structure. Bond-valence calculations indicate that the

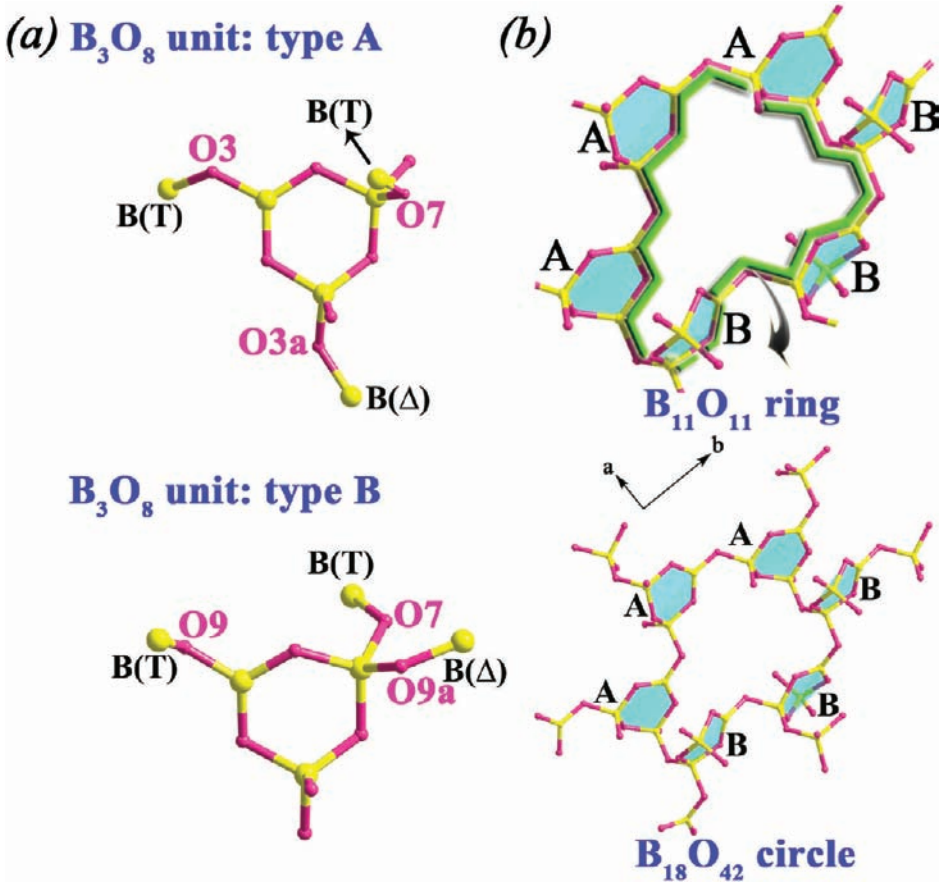

Figure 2. (a) Two kinds of spatial connections of the B_3O_8 units: type A and type B. (b) Perspective views of the $B_{11}O_{11}$ ring and $B_{18}O_{42}$ circle within the anion layer.

dx.doi.org/10.1021/ic2021337 | *Inorg. Chem.* 2012, 51, 1852−1858

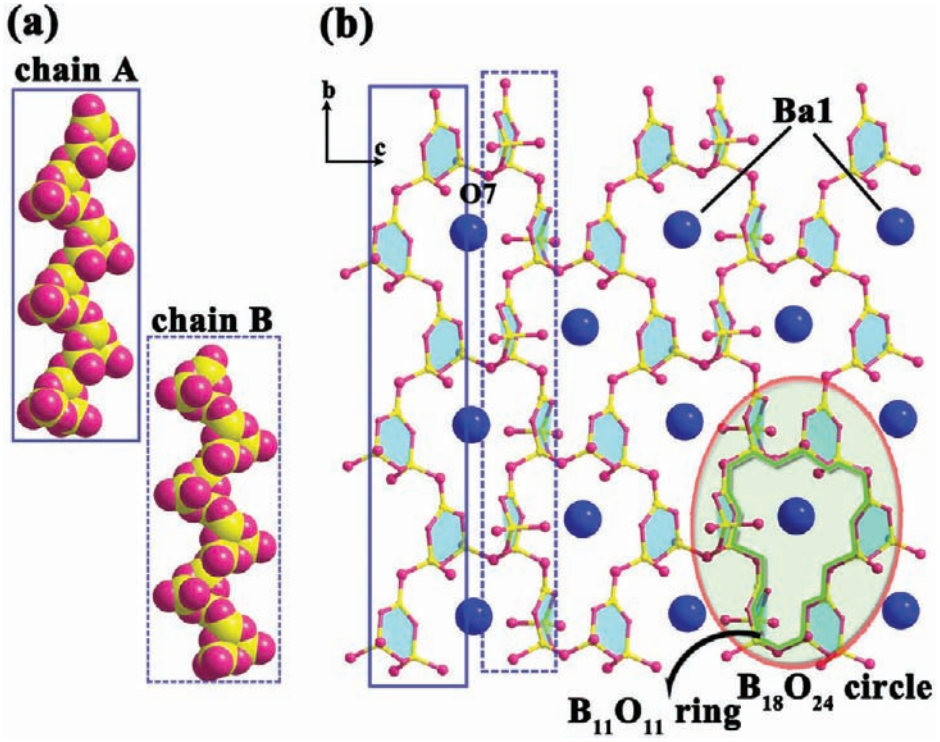

Figure 3. (a) Space-filling model representing two kinds of helical chain structures of $Ba_2[B_6O_9(OH)_4]$ along the *bc* and *ab* planes. (b) Homochiral layer run parallel to *bc* plane, showing the homochirality transfer through O7 atoms connection between neighboring helical chains. The Ba1 atom is located in the cavity surrounded by the $B_{11}O_{11}$ ring within the anion layer.

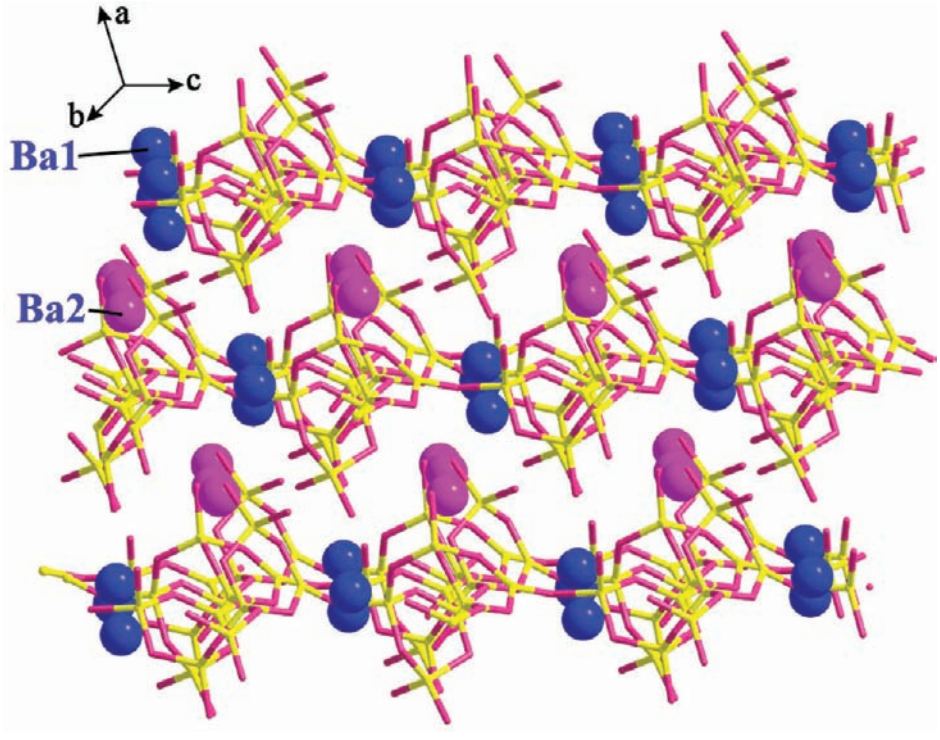

Figure 4. Perspective of the 3D stacking structure of $Ba_2[B_6O_9(OH)_4]$.

calculated total bond valences for B1, B2, B3, B4, B5, and B6 are 3.01, 2.96, 3.03, 3.02, 3.07, and 3.03, respectively; the valences for Ba1 and Ba2 are 2.17 and 2.00.[23]

We compare the crystal structure of $Ba_2[B_6O_9(OH)_4]$ with $NaNd[B_6O_9(OH)_4]$ prepared by Belokonova et al.[24] Different from $Ba_2[B_6O_9(OH)_4]$, which crystallizes in the noncentrosymmetric space group $P2_1$, $NaNd[B_6O_9(OH)_4]$ crystallizes in the centrosymmetric space group $P-1$. Furthermore, $Ba_2[B_6O_9(OH)_4]$ contains infinite layers extended by the B_3O_8 units made up of one BO_3 triangle (Δ) and two BO_4

dx.doi.org/10.1021/ic2021337 | *Inorg. Chem.* 2012, 51, 1852–1858

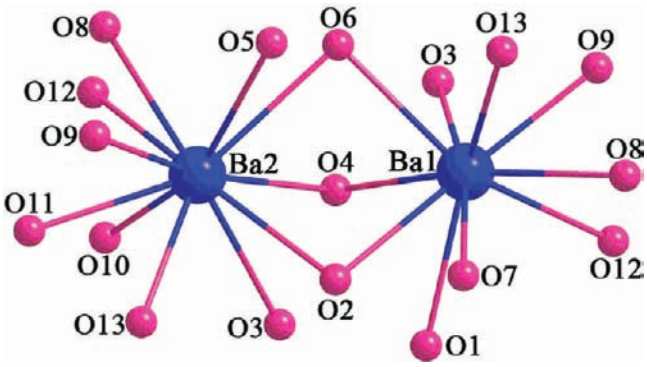

Figure 5. Coordination environment of two kinds of Ba atoms.

tetrahedra (T) with vertex-sharing O atoms along the *ab* plane. Yet $NaNd[B_6O_9(OH)_4]$ contains a 1D anionic chain with the formula 6: [4T+2Δ] which was built as corner-sharing BO_4 tetrahedra united by pseudoaxis 3_1 into a helical chain; the chain is lined with two BO_3 triangles and one tetrahedron BO_4 linked through their corners. Last, the Ba1 atom of $Ba_2[B_6O_9(OH)_4]$ is coordinated by 10 O atoms and the Ba2 atom is coordinated by 11 O atoms, while the Na atom of $NaNd[B_6O_9(OH)_4]$ is coordinated by 7 oxygen atoms and Nd by 9 oxygen atoms.

Infrared Spectroscopy. The spectrum exhibited the following absorption peaks, which are assigned referring to the literature (Figure S2, Supporting Information).[25] The peaks at 3137, 3474, and 3534 cm^{-1} can be attributed to the presence of hydroxyl groups. The peaks at 1318 and 1172 cm^{-1} can be attributed to asymmetric stretching and symmetric stretching vibrations of BO_3 groups, respectively. The bands of 916, 726, and 793 cm^{-1} are likely the asymmetric and symmetric stretching of B−O in BO_4. The deformation vibration at 580 cm^{-1} can be assigned as the bending of BO_3 groups and 520 cm^{-1} to the bending mode of BO_4 groups.

UV−Vis Diffuse Reflectance Spectroscopy. The UV−vis diffuse reflectance spectrum for $Ba_2[B_6O_9(OH)_4]$ is shown in Figure S3, Supporting Information. Absorption (K/S) data are calculated from the following Kubelka−Munk function

$$F(R) = \frac{(1-R)^2}{2R} = \frac{K}{S}$$

where R is the reflectance, K is the absorption, and S is the scattering.[26] Obviously, it has a cutoff edge below 190 nm, indicating that the optical crystal may have potential use in deep UV NLO applications.

TGA/DSC. The results of the thermal analyses are represented by the curves in Figure S4, Supporting Information. From the TGA curve it can be seen that the material is very stable and there is no weight loss when the temperature is lower than 400 °C. Then, it undergoes a weight loss between ca. 420 and 480 °C because of the release of the two molecules of H_2O. The observed weight loss of 6.45% matches well with the calculated one (6.52%). In the second stage, occurring between 498 and 600 °C, the weight loss might be attributed to the gradual volatilization of boron oxide. The DTA curve of $Ba_2[B_6O_9(OH)_4]$ is consistent with the above deductions. The endothermic peak at 438 °C corresponds to loss of two water molecules.

NLO Properties. Since $Ba_2[B_6O_9(OH)_4]$ crystallizes in the noncentrosymmetric space group $P2_1$, it is worthy to study its SHG properties. Single crystals grown by the hydrothermal method were ground into powder with different sizes and loaded into a quartz cell. Phase-matching experiments, that is, particle size vs SHG efficiency, indicate that the crystals of $Ba_2[B_6O_9(OH)_4]$ are phase matchable, having a powder SHG effect about 3 times that of KDP standard of similar grain size (Figure 6).

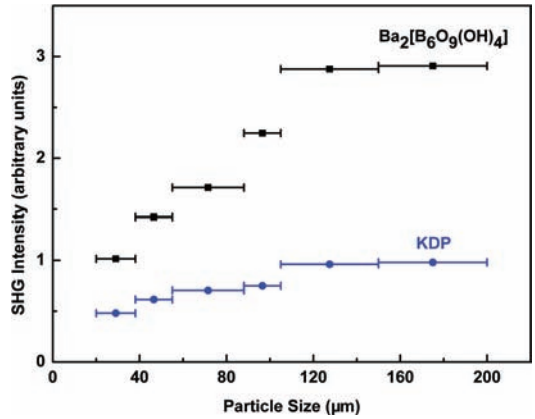

Figure 6. SHG measurements of $Ba_2[B_6O_9(OH)_4]$ ground crystals with KDP as a tester.

To analyze the structure−property relation of $Ba_2[B_6O_9(OH)_4]$, the direction and magnitude of the distortion in BaO_n (n = 10, 11) polyhedra and BO_3 triangles have been quantified by determining the local dipole moments. This method uses a bond-valence approach to calculate the direction and magnitude of the dipole moment.[27] The well-known Debye equation, $\mu = neR$[27a] (μ is the net dipole moment in Debye (10^{-18} esu cm), n the total number of electrons, e the charge on an electron, -4.8×10^{-10} esu, and R the difference, in cm, between the "centroids" of positive and negative charge), has been used to calculate the dipole moment of individual Ba−O and B−O bonds. Distribution of the electrons on the Ba/O/B atoms were estimated using bond-valence theory ($S_i = \exp[(R_o - R_i)/B]$, where R_o is an empirical constant, R_i is the length of bond i (in ANgstroms), and B = 0.37).[23] These bond-valence calculations have been previously used to understand the distortion of MoO_6 octahedra and TeO_x (x = 3, 4) polyhedra in $BaTeMo_2O_9$,[27e] acentric $MoO_3F_3^{3-}$ anions in $(Ag_3MoO_3F_3)$-$(Ag_3MoO_4)Cl$,[27a] as well as other polyhedras of oxidate, etc.,[27] and well explain the experimental results. The entire calculation process has been described in detail in the Supporting Information of ref 27e.

Using this methodology, we calculate the dipole moment of BaO_n (n = 10, 11) polyhedra and BO_3 triangles in $Ba_2[B_6O_9(OH)_4]$. In the calculation of distortion, BO_4 is neglected owing to its small contribution to SHG according to the anionic group theory of NLO activity in borates.[28] The total polarization of $Ba_2[B_6O_9(OH)_4]$ in the unit cell and the contributions from BO_3 groups and BaO_n (n = 10,11) polyhedra to the total polarization have been shown in Table 3. It is clear that the magnitudes of dipole moments along the a and c axes are canceled and the vector sum of them is well enhanced along the negative b axis (Figure 7), which leads to the large SHG response of $Ba_2[B_6O_9(OH)_4]$.

dx.doi.org/10.1021/ic2021337 | Inorg. Chem. 2012, 51, 1852−1858

Table 3. Direction and Magnitude of the Distortion of the BO_3 Triangle and BaO_n (n = 10, 11) Polyhedra in $Ba_2[B_6O_9(OH)_4]$

		dipole moment			
					magnitude
species	symmetric code	x	y	z	debye
$Ba(1)O_{10}$	x, y, z	−0.6921	−0.3300	1.0521	1.4011
$Ba(1a)O_{10}$	$1 - x, 0.5 + y, 1 - z$	0.6925	−0.3296	−1.0517	
$Ba(2)O_{11}$	x, y, z	−0.2506	−0.9379	−2.5129	2.6505
$Ba(2a)O_{11}$	$1 - x, -0.5 + y, 1 - z$	0.2511	−0.9381	2.5138	
$B(2)O_3$	x, y, z	0.5765	−0.1838	−0.3882	0.7741
$B(2a)O_3$	$1 - x, -0.5 + y, 1 - z$	−0.5767	−0.1862	0.3883	
$B(5)O_3$	$2 - x, 0.5 + y, 2 - z$	−0.8849	−0.4463	−0.1230	0.9784
$B(5a)O_3$	$-1 + x, y, -1 + z$	0.8861	−0.4453	0.1230	
unit cell		0	−3.7972	0	

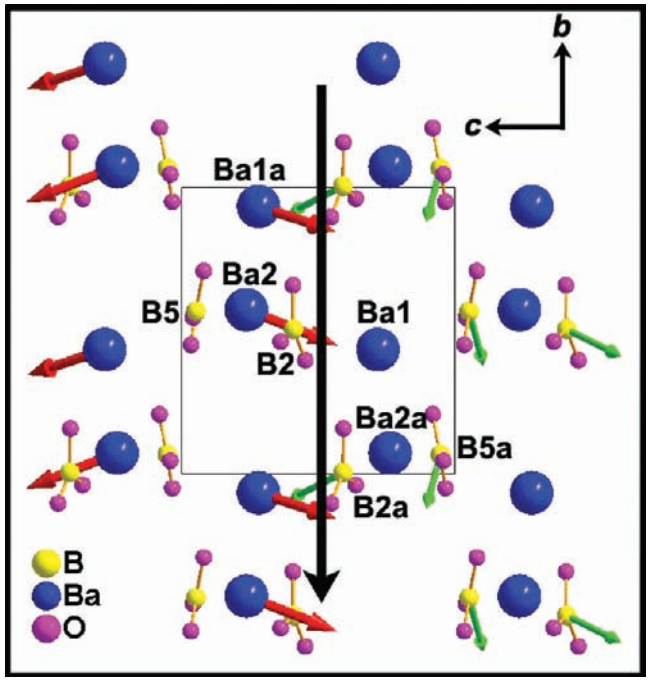

Figure 7. Ball-and-stick representation of the BO_3 triangle and BaO_n (n = 10, 11) polyhedra. Red and green arrows indicate the approximate direction of the distortions for the BaO_n and BO_3 triangle, respectively. Black arrow represents the direction of the net distortion for $Ba_2[B_6O_9(OH)_4]$.

CONCLUSION

In summary, a new barium polyborate, $Ba_2[B_6O_9(OH)_4]$, is acquired under hydrothermal conditions for the first time. It contains a unique chiral layer $[B_6O_9(OH)_4]_n^{4n-}$ featuring novel $B_{18}O_{42}$ circles based on B_3O_8 circles [(3: Δ+2T)] in an AAABBB manner. The compound possesses a UV cutoff edge below 190 nm. It is type I phase matchable and exhibits an SHG efficiency of about 3 times that of KDP. The NLO effect originates from the cooperative effect of BO_3 groups and strong distortions of barium oxygen polyhedra in this system. These features make $Ba_2[B_6O_9(OH)_4]$ very promising as deep UV NLO materials for practical applications. Continuing efforts are underway to find new NLO materials in order to understand the structural nature of their polarity and to characterize their functional properties.

ASSOCIATED CONTENT

Supporting Information

CIF file, tables of atomic coordinates, bond angles, calculated, and observed XRD patterns, infrared spectroscopy, UV−vis diffuse-reflectance spectrum, TGA/DSC curve, etc. This material is available free of charge via the Internet at http://pubs.acs.org.

AUTHOR INFORMATION

Corresponding Author

*Phone: (86)991-3674558. Fax: (86)991-3838957. E-mail: slpan@ms.xjb.ac.cn.

ACKNOWLEDGMENTS

This work was supported by the Main Direction Program of Knowledge Innovation of Chinese Academy of Sciences (grant nos. KJCX2-EW-209-3 and KJCX2-EW-H03-03), the "National Natural Science Foundation of China" (grant nos. 50802110, 21001114, and 21065012), the "One Hundred Talents Project Foundation Program" of the Chinese Academy of Sciences, the "Western Light Joint Scholar Foundation" Program of the Chinese Academy of Sciences, the "High Technology Research and Development Program" of Xinjiang Uygur Autonomous Region of China (grant no. 201116143), the Natural Science Foundation of Xinjiang Uygur Autonomous Region of China (grant nos. 200821159 and 2009211B33), and Scientific Research Program of Urumqi of China (grant no. G09212001), as well as the Science and Technology in Support of Xinjiang (grant no. 201091244). The authors also thank Professor Ming-hua Zeng for help with the structure relationship of $Ba_2[B_6O_9(OH)_4]$.

REFERENCES

(1) (a) Halasyamani, P. S.; Poeppelmeier, K. R. *Chem. Mater.* **1998**, *10*, 2753. (b) Hagerman, M. E.; Poeppelmeier, K. R. *Chem. Mater.* **1995**, *7*, 602. (c) Marvel, M. R.; Lesage, J.; Baek, J.; Halasyamani, P. S.; Stern, C. L.; Poeppelmeier, K. R. *J. Am. Chem. Soc.* **2007**, *129*, 13963. (d) Maggard, P. A.; Stern, C. L.; Poepplemeier, K. R. *J. Am. Chem. Soc.* **2001**, *123*, 7742.

(2) (a) Chang, H. Y.; Kim, S. H.; Ok, K. M.; Halasyamani, P. S. *J. Am. Chem. Soc.* **2009**, *131*, 6865. (b) Halasyamani, P. S.; O'Hare, D. *Chem. Mater.* **1998**, *10*, 646. (c) Halasyamani, P. S. *Chem. Mater.* **2004**, *16*, 3586. (d) Halasyamani, P. S.; Francis, R. J.; Walker, S. M.; O'Hare, D. *Inorg. Chem.* **1999**, *38*, 271.

(3) Becker, P. *Adv. Mater.* **1998**, *10*, 979.

(4) (a) Sun, C. F.; Hu, C. L.; Xu, X.; Yang, B. P.; Mao, J. G. *J. Am. Chem. Soc.* **2011**, *133*, 5561. (b) Kong, F.; Huang, S. P.; Sun, Z. M.; Mao, J. G. *J. Am. Chem. Soc.* **2006**, *128*, 7750. (c) Zhang, J. H.; Hu, C.

L.; Xu, X.; Fang, K.; Mao, J. G. *Inorg. Chem.* **2011**, *50*, 1973. (d) Zhang, J. D.; Kong, F.; Mao, J. G. *Inorg. Chem.* **2011**, *50*, 3037. (e) Kong, F.; Jiang, H. L.; Hu, T.; Mao, J. G. *Inorg. Chem.* **2008**, *47*, 10661. (f) Mao, J. G.; Jiang, H. L.; Fang, K. *Inorg. Chem.* **2008**, *47*, 8498.

(5) (a) Zhang, W. L.; Chen, W. D.; Zhang, H.; Geng, L.; Lin, C. S.; He, Z. Z. *J. Am. Chem. Soc.* **2010**, *132*, 1508. (b) Wang, S. C.; Ye, N.; Li, W.; Zhao, D. *J. Am. Chem. Soc.* **2010**, *132*, 8779. (c) Huang, Y. Z.; Wu, L. M.; Wu, X. T.; Li, L. H.; Chen, L.; Zhang, Y. F. *J. Am. Chem. Soc.* **2010**, *132*, 12788.

(6) (a) Wu, H. P.; Pan, S. L.; Poeppelmeier, K. R.; Li, H. Y.; Jia, D. Z.; Chen, Z. H.; Fan, X. Y.; Yang, Y.; Rondinelli, J. M.; Luo, H. S. *J. Am. Chem. Soc.* **2011**, *133*, 7786. (b) Pan, S. L.; Smit, J. P.; Watkins, B.; Marvel, M. R.; Stern, C. L.; Poeppelmeier, K. R. *J. Am. Chem. Soc.* **2006**, *128*, 11631. (c) Li, F.; Hou, X. L.; Pan, S. L.; Wang, X. A. *Chem. Mater.* **2009**, *21*, 2846. (d) Pan, S. L.; Wu, Y. C.; Fu, P. Z.; Zhang, G. C.; Li, Z. H.; Du, C. X.; Chen, C. T. *Chem. Mater.* **2003**, *15*, 2218. (e) Yang, Y.; Pan, S. L.; Hou, X. L.; Wang, C. Y.; Poeppelmeier, K. R.; Chen, Z. H.; Wu, H. P.; Zhou, Z. X. *J. Mater. Chem.* **2011**, *21*, 2890.

(7) (a) Choyke, S. J.; Blau, S. M.; Larner, A. A.; Narducci Sarjeant, A.; Yeon, J.; Halasyamani, P. S.; Norquist, A. J. *Inorg. Chem.* **2009**, *48*, 11277. (b) Hubbard, D. J.; Johnston, A. R.; Sanchez Casalongue, H.; Narducci Sarjeant, A.; Norquist, A. J. *Inorg. Chem.* **2008**, *182*, 8518.

(8) Chen, C. T.; Wu, B. C.; Jiang, A. D.; You, G. M. *Sci. Sin. B* **1985**, *28*, 235.

(9) Chen, C. T.; Wu, Y. C.; Jiang, A. D.; You, G. M.; Li, R. K.; Lin, S. J. *J. Opt. Soc. Am. B* **1989**, *6*, 616.

(10) Wu, Y.; Sasaki, T.; Nakai, S.; Yokotani, A.; Tang, H.; Chen, C. *Appl. Phys. Lett.* **1993**, *62*, 2614.

(11) Mori, Y.; Kuroda, I.; Nakajima, S.; Sasaki, T.; Nakai, S. *Appl. Phys. Lett.* **1995**, *67*, 1818.

(12) Chemla, D. S.; Kupecek, P. J.; Robertson, D. S.; Smith, R. C. *Opt. Commun.* **1971**, *3*, 29.

(13) *SAINT*, version 7.60A; Bruker Analytical X-ray Instruments, Inc.: Madison, WI, 2008.

(14) Sheldrick, G. M. *SHELXTL*, version 6.14; Bruker Analytical X-ray Instruments, Inc.: Madison, WI, 2003.

(15) Spek, A. L. *J. Appl. Crystallogr.* **2003**, *36*, 7.

(16) (a) Kurtz, S. K.; Perry, T. T. *J. Appl. Phys.* **1968**, *39*, 3798. (b) Dougherty, J. P.; Kurtz, S. K. *J. Appl. Crystallogr.* **1976**, *9*, 145.

(17) Christ, C. L.; Clark, J. P. *Phys. Chem. Mineral.* **1977**, *2*, 59.

(18) Touboul, M.; Penin, N.; Nowogrocki, Guy. *Solid State Sci.* **2003**, *5*, 1327.

(19) Wu, Y. C.; Liu, J. G.; Fu, P. Z.; Wang, J. X.; Zhou, H. Y.; Wang, G. F.; Chen, C. T. *Chem. Mater.* **2001**, *13*, 753.

(20) Yu, Z. T.; Shi, Z.; Jiang, Y. S.; Yuan, H. M.; Chen, J. S. *Chem. Mater.* **2002**, *14*, 1314.

(21) Li, L. Y.; Li, G. B.; Wang, Y. X.; Liao, F. H.; Lin, J. H. *Chem. Mater.* **2005**, *17*, 4174.

(22) (a) Fan, X. Y.; Pan, S. L.; Hou, X. L.; Liu, G.; Wang, J. D. *Inorg. Chem.* **2009**, *48*, 4806. (b) Wang, Y. J.; Pan, S. L.; Hou, X. L.; Zhou, Z. X.; Liu, G.; Wang, J. D.; Jia, D. Z. *Inorg. Chem.* **2009**, *48*, 7800. (c) (d) Fan, X. Y.; Pan, S. L.; Hou, X. L.; Tian, X. L.; Han, J.; Haag, J.; Poeppelmeier, K. R. *Cryst. Growth Des.* **2010**, *10*, 252. (e) Li, F.; Pan, S. L.; Hou, X. L.; Yao, J. *Cryst. Growth Des.* **2009**, *9*, 4091.

(23) (a) Brown, I. D.; Altermatt, D. *Acta Crystallogr.* **1985**, *B41*, 244. (b) Brese, N. E.; O'Keeffe, M. *Acta Crystallogr.* **1991**, *B47*, 192.

(24) Belokoneva, E. L.; Ivanova, A. G.; Dimitrova, O. V. *Russ. J. Inorg. Chem.* **2006**, *51*, 869.

(25) Li, J.; Xia, S.; Gao, S. *Spectrochim. Acta* **2005**, *433*, 196.

(26) (a) Kubelka, P.; Munk, F. *Z. Tech. Phys.* **1931**, *12*, 593. (b) Tauc, J. *Mater. Res. Bull.* **1970**, *5*, 721.

(27) (a) Maggard, P. A.; Nault, T. S.; Stern, C. L.; Poeppelmeier, K. R. *J. Solid State Chem.* **2003**, *175*, 27. (b) *Inorg. Chem.* **2005**, *44*, 3919. (c) Izumi, H. K.; Kirsch, J. E.; Stern, C. L.; Poeppelmeier, K. R. *Inorg. Chem.* **2005**, *44*, 884. (d) Kim, J. H.; Halasyamani, P. S. *J. Solid State Chem.* **2008**, *181*, 2108. (e) Zhang, J. J.; Zhang, Z. H.; Zhang, W G; Zheng, Q. X.; Sun, Y. X.; Zhang, C. Q.; Tao, X. T. *Chem. Mater.* **2011**, *23*, 3752.

(28) Chen, C. T.; Wu, Y. C.; Li, R. C. *J. Cryst. Growth* **1990**, *99*, 790.